W. Thomas Dixon, Ph.D.

Simple Proton Spectroscopic Imaging[1]

Simple modification of a spin echo imaging pulse sequence generates useful spectroscopic information at 0.35 T. New images are produced that show water only, fat only, and the difference between water and fat intensity. Imaging speed, spatial resolution, and signal-to-noise ratio are comparable with ordinary imaging. The method provides new parameters for tissue characterization and improved contrast between some organs.

Index terms: Magnetic resonance, spectroscopy • Magnetic resonance, technology

Radiology 1984; 153: 189-194

MAGNETIC resonance (MR), one of the most widely used spectroscopic techniques, is now a rapidly growing imaging technique as well. There are several MR techniques that combine spectroscopy with imaging (1-9). These have been demonstrated on the nuclei of hydrogen (1, 5, 7-9), deuterium (3), carbon (5), and P-31 (2, 4, 6).

There is a great deal to be learned from these techniques. For example, in an imaging experiment, the P-31 spectrum, which has about 6 lines, can show regional pH and concentrations of ATP, phosphocreatine, and inorganic phosphate simultaneously. Complicated results like this are usually presented as spectra from specified regions in an organism rather than as images at specified chemical shifts.

Since most of the total nuclear magnetization in a body comes from protons in water, and most of what is left, from protons in fat, an unsophisticated approach may skim off a good fraction of the possible benefits of spectroscopy at low cost. The technique demonstrated here simply separates an image at the water chemical shift from one at the CH_2 chemical shift.

This simple technique is able to maintain an image spatial resolution, signal-to-noise ratio, and acquisition time similar to conventional MR images for two reasons. First, water and fat give good signal-to-noise ratios because they are much more abundant than other potentially interesting metabolites. Second, an undesirable trade-off between spatial resolution and imaging time is avoided by leaving a magnetic field gradient on during signal acquisition. It is necessary to repeat a pulse sequence once for each voxel imaged if the gradients are off during acquisition. Since repetition times of at least one-half T1 are desirable (10), imaging on a 256 × 256 matrix takes a long time (256^2 seconds is more than 18 hours). This trade-off would not be such a problem imaging less abundant metabolites. There, to get sufficient signal-to-noise ratio for an image, long imaging times and larger, therefore fewer, voxels are needed whether the gradient is left on or off.

Numerous advantages are expected from adding spectroscopy to imaging. Comparing images using new gray scales with conventional T1 or T2 weighted images helps to identify tissues, even if the principles of the new scales are not understood. Here, however, the new gray scales depend on a very familiar chemical parameter, fat content.

The contrast between fat-containing tissues and others may be increased in spectroscopic imaging, allowing detection of smaller masses of or in fat-containing tissue.

Spectroscopy is obviously a help in efforts to identify tissue from measured parameters rather than image appearance, since it introduces more parameters (*e.g.*, T1 of fat, T1 of water). Since T1 values now reported are a weighted average of fat and water T1 values, spectroscopy can also eliminate one source of method dependence in the results of parameter measurements. This will make it easier to compare results obtained in different hospitals.

Finally, the image of the fat and the image of the water in an ordinary MR image are not perfectly registered, thus degrading edge definition. This gets worse as fields are raised or gradients are lowered

[1] From the Mallinckrodt Institute of Radiology, Washington University School of Medicine, St. Louis, MO. Presented at the Sixty-ninth Scientific Assembly and Annual Meeting of the Radiological Society of North America, Chicago, IL, Nov. 13-18, 1983. Received Dec. 15, 1983, revision requested March 19, 1984; revision received and accepted May 3, 1984.

See also the paper by Lee *et al.* (pp. 195-201) in this issue.

ht

Figure 1

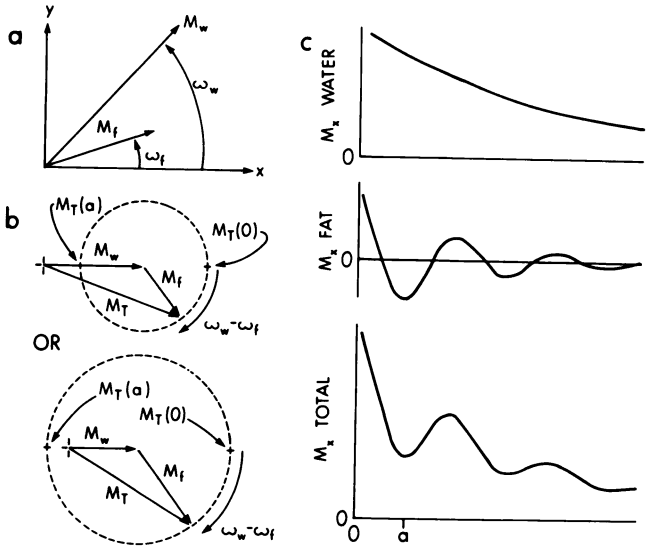

Transverse magnetization following a 90° pulse. The volume element contains both water and fat. M_w = water magnetization; M_f = fat magnetization; ν_w and ν_f = Larmor frequencies of water and fat ($\omega = 2\pi\nu$).

a. Laboratory frame.

b. Rotating frame, top $|M_w| > |M_f|$, bottom $|M_f| > |M_w|$.

c. Typical FID.

Figure 2

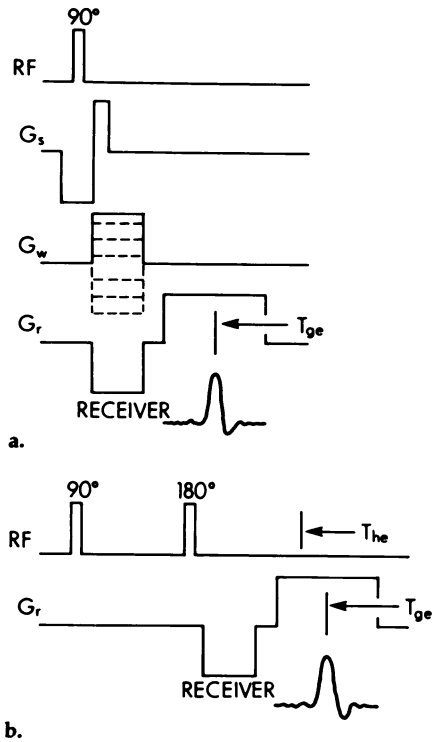

Pulse sequences. G_s = section selection gradient; G_w = warp or phase encoding gradient; G_r = read out gradient.

a. Basic spin warp sequence.

b. Spin warp with spin echo.

in an effort to improve signal-to-noise ratio. Spectroscopically separated images can be shifted back into register, improving edge definition.

EQUIPMENT

The experiments described here were performed on a Siemens Magnetom with a 1-meter bore Oxford magnet operating at 0.35 T. Gradients are 1.5 mT/m or 50 Hz/mm. No special shimming was used for spectroscopy.

THEORY

At the end of a 90° pulse, or at a Hahn spin echo (11), the magnetization of the protons in water and the magnetization of protons in fat CH_2 groups point in the same direction. This situation does not last, since the water protons precess between 3 and 4 parts per million faster than the fat protons (Fig. 1a). This difference is about 50 Hz at 0.35 T.

The total magnetization is the vector sum of the water and fat magnetization as illustrated in Figure 1b. This figure is drawn in a frame rotating at the water proton frequency. It shows that the total magnetization is initially a maximum when water and fat magnetization point in the same direction but soon goes through a minimum when water and fat magnetization point in opposite directions. This behavior is repetitive at the difference between the water and fat proton frequencies.

The variations in the total magnetization shown in Fig. 1b lead to periodic variations in the free induction signal of Fig. 1c. The first minimum of Fig. 1c will occur when

$$t = \frac{1}{2(\nu_w - \nu_f)} \equiv a$$

The time is t and ν_w and ν_f are water and fat proton frequencies.

The time a is important because an ordinary imaging sequence "done" at the minimum, $t = a$, results in a new type of image. In this image the brightness of a pixel depends on the difference between the water and fat magnetizations. An ordinary image taken at the maximum, $t = 0$, shows the sum of water and fat magnetization[2]. Both images are useful in their own right but their sum and difference are also useful. The sum is an image of water only, the difference of fat. These four images will be referred to as in-phase (or conventional), opposed, water, and fat images, respectively. Components less abundant than water and fat contribute some intensity to both the water and fat images as well as to the in-phase image.

The arguments presented so far do not depend on the details of any specific imaging technique and this paper will not explain how imaging itself works. Figure 2 shows how these general spectroscopic principles can be implemented in spin-warp imaging (13, 14). The basic sequence is illustrated in Fig. 2a. Consider first a perfectly homogeneous field, a pure water object, and an instrument tuned to the Larmor frequency of water. The 90° pulse in the presence of the gradient G_s excites a plane of water. G_w, the warp gradient, identifies spins according to their location along the warp axis. The warp, or phase encoding gradient, has nothing to do with spectroscopy and won't be considered further.

The read gradient, perpendicular to the other two, relates the frequency of a spin, a measurable quantity, to its location along the read gradient axis.

Data collection starts either when the read gradient, G_r, is turned on or else at a gradient echo that can be described as follows: If the magnetization vectors of all voxels are initially

[2] Data collection at times other than 0 or a gives intermediate results. For example, 7 msec after a 90° pulse at a field of 0.15 T (normal operation for Picker International [12]) the water and fat signals would be about 55° out of phase. In the most sensitive case, water and fat magnetizations equal, this results in a pixel value about 10% less than the sum of water and fat magnetization.

aligned, the gradient fans them out in different directions so that the total magnetization and nuclear induction signal disappear. Reversing the direction of the gradient reverses the motion of each vector so they eventually realign and an echo occurs. This occurs at a time T_{ge} when

$$\int_0^t G_r(t)dt = 0$$

so all effects of the gradient have been cancelled.

Most images are made in a spin echo mode using a 180° pulse to give a Hahn spin echo (11). At the Hahn echo (Fig. 2b) all effects of chemical shift differences and magnetic field inhomogeneities are completely cancelled. If $T_{ge} = T_{he}$ the image is made with water and fat spins aligned ($t = 0$ for Fig. 1) and an image of water plus fat results. If $T_{ge} = T_{he} \pm a$ the water and fat spins point in opposite directions so the image shows the difference between water and fat magnetization.

Modifications of a standard Siemens spin-echo pulse sequence were used for this paper. Two time delays were changed but no change in the order or number of events was required. If you are designing a pulse sequence from scratch, rather than modifying a commercial one, keep in mind that the effect of any gradient after the 180° refocusing pulse is exactly opposite in sign to what it would be if applied before the 180° pulse. In Siemens and most other commercial instruments data are collected both before and after the gradient echo rather than just after it (15). This difference should not affect spectroscopy.

Figure 3

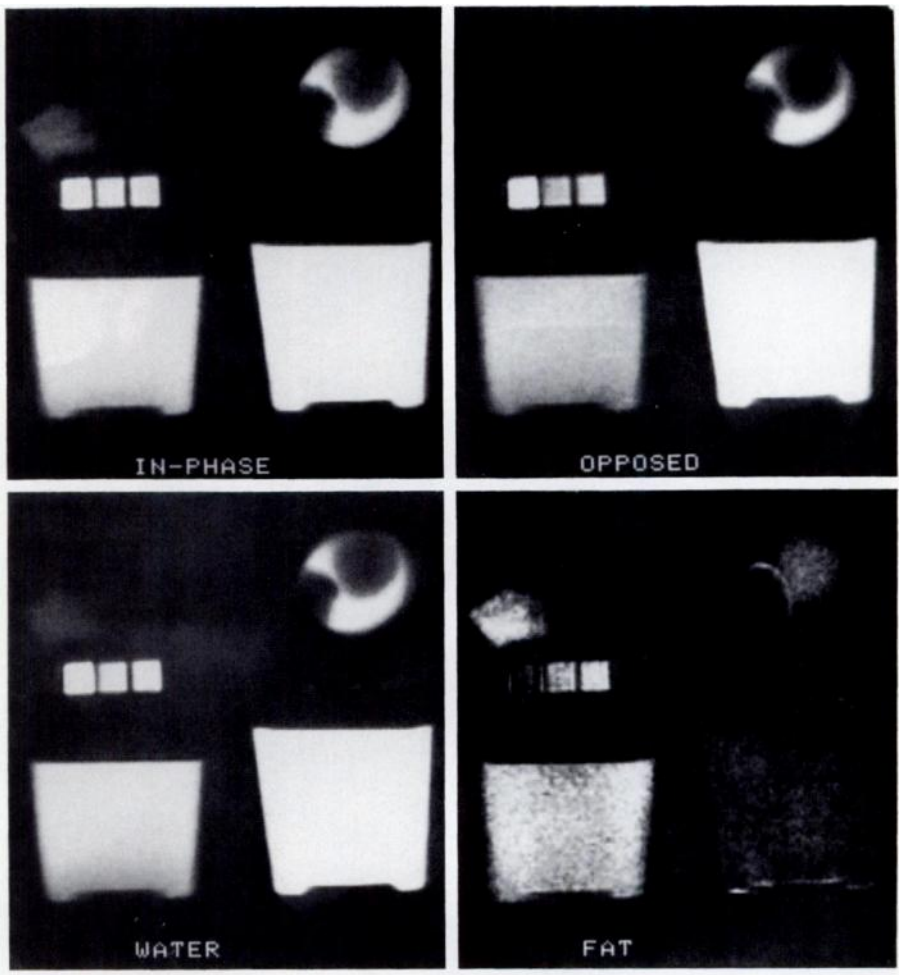

Spectroscopic images. The material above the three squares is Bluebonnet Margarine (Nabisco). Below is Dawn detergent (Proctor and Gamble). The hen's egg is above a container of 0.1% $CuSO_4$ in water. The doped water container has no fat in it so it is bright on the water image but nearly invisible on the fat image. The detergent appears on all images; its relative brightness on the water and fat images depends on the relative concentration of aliphatic and water protons and on the T1 and T2 values. The margarine is faint because it is fairly solid and so has a short fat T2 value, and it contains little water. In three of the images of the egg, both the yolk and white are visible, but in the fat image only the yolk is visible, showing that egg white does not contain fat but the yolk does.

RESULTS

The results of this technique are presented as sets of four images. In each case the upper left is a conventional 40-msec spin echo. An opposed image, which has the 180° pulse 5 msec earlier, is in the upper right. At the lower left is the water image, the sum of the upper two. The fat image at the lower right is the conventional less the opposed image. The window setting (camera brightness) is adjusted individually for each image. The fat image is usually made brighter than the others.

All sections are 10 mm thick, pixels are approximately 2 mm square, and repetition times were 1.4 or 1.5 seconds. Two averages are used for the in-phase and the opposed images. The images have been cropped from a 256 × 256 matrix.

The bottom of Figure 3 demonstrates this type of spectroscopy most clearly. The doped water container has no fat so it is bright on the water image but nearly invisible on the fat image. The intensity that remains may come from electronic drift during imaging.

The detergent appears on all images. Its relative brightness on the water and fat images depends on the relative concentration of aliphatic and water protons (27% aliphatic balance water on a 60-MHz spectrum) and on the aliphatic and water T1 and T2 values, which were not measured.

The margarine is faint because it is fairly solid and so has a short fat T2 (evidently less than 40 msec) and it contains little water. Its disappearance from the opposed image indicates water and fat magnetizations are about the same under these experimental conditions.

The hen's egg is the most interesting object. In three of the images yolk and white are visible but in the fat image only the yolk is visible. One concludes egg white does not contain fat but yolk does.

Figure 4 is a transverse section through the kidneys. There are two striking differences between the in-phase and opposed images. First, in the opposed images the boundaries between most organs are clearly delineated by dark lines of fat, in fact, these boundaries are almost the only thing visible in the fat image. Second, the parenchyma of the kidneys seems brighter than in the conventional image. The left kidney is much easier to see in the opposed than in the in-phase image. Since nothing can be more intense in the opposed than in the in-phase image, most other tissues are actually darkened. This darkening could be caused by a small amount of

Figure 4

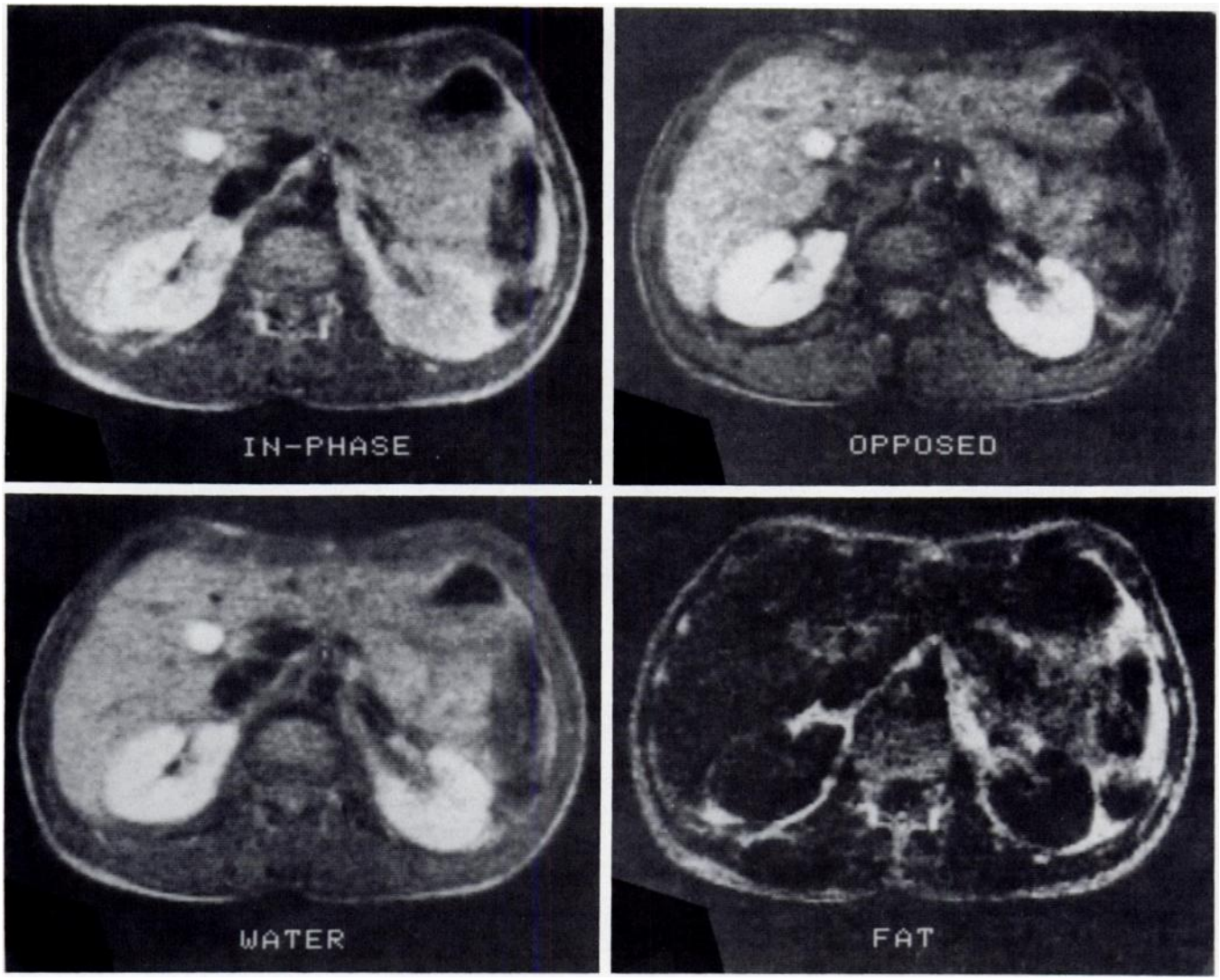

Transverse images of a normal volunteer after a 20-hour fast. In the opposed image the boundaries between most organs are clearly delineated by dark lines of fat. The parenchyma of the kidneys seems brighter in the opposed image than in the conventional image. The left kidney is much easier to see in the opposed than in the in-phase image. Note that the gallbladder has visible intensity in the fat image, even though bile should be 90% water. The spinal canal is more easily seen in the opposed than in the conventional image.

fat or, especially in the liver, by a larger amount of glycogen or soluble proteins.

Notice that after a 20-hour fast the gall bladder has visible intensity in the fat image even though bile should be 90% water. The spinal canal is more easily seen in the opposed than in the conventional image.

The appearance of subcutaneous fat deserves special attention in these images. The subcutaneous fat in the back is not dark in the opposed image and appears in the water image rather than the fat image. In the front this is not a problem. A more caudal section (Fig. 5) shows more complete transfer of subcutaneous fat from the fat image to the water image. The opposed image has dark stains along the surfaces of the muscles.

DISCUSSION

Figures 3–5 demonstrate that proton spectroscopic images can be made with ordinary spatial resolution. As predicted in theory this can be done without large increases in magnetic field strength or homogeneity, or in imaging time. Spectroscopy results in the useful and unexpected examples of increased tissue discrimination mentioned under Results. There are some properties and problems of this technique and its resulting images that are not immediately obvious from glancing at the figures.

The worst problem with this method comes from magnetic field inhomogeneities which, over a whole image, are many times as large as the chemical shift difference between water and fat. During the time a, the direction (phase) of the magnetization changes drastically, making it impossible to get a water or fat image by simple addition and subtraction. Also the original opposed image itself, where $T_{ge} \neq T_{he}$, has terrible phase distortions. The solution used here was to take the absolute value of the complex images before subtraction. While this costs the usual $\sqrt{2}$ in signal-to-noise ratio, it is very easy since most imager manufacturers present only absolute-value images anyway.

This absolute value causes the same type of problem in opposed images that it does in inversion recovery images. In an inversion recovery image a bright area represents either a region with a very short or a very long T1, but one can't tell which. In opposed images

Figure 5

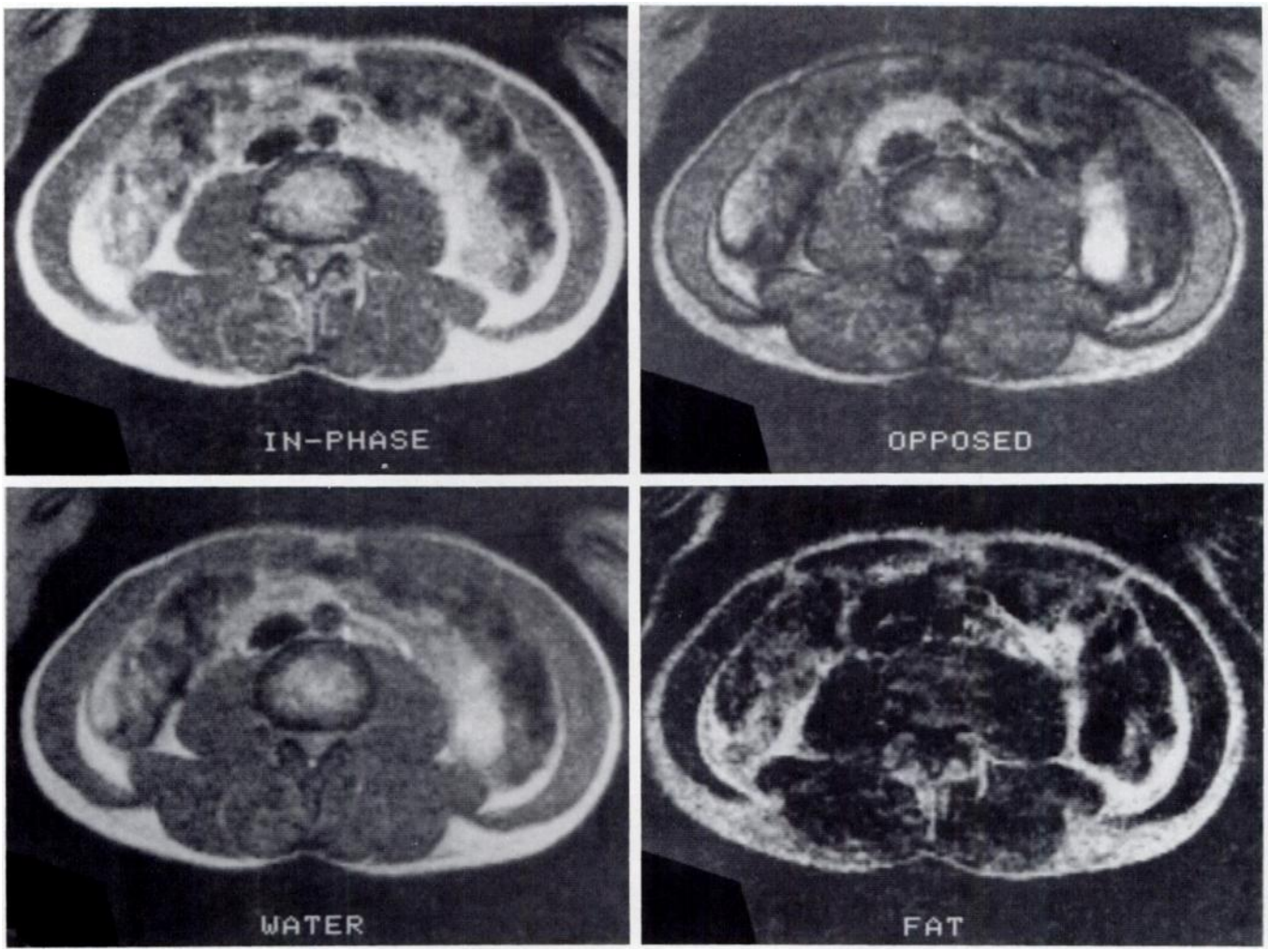

Images of a plane 40 mm caudal to Figure 4. Both sets of images were made at the same time using multiple section capability. Note that in both figures the subcutaneous fat in the back is not dark in the opposed image and appears in the water image rather than the fat image. In the front this is not a problem.

both regions with no fat and regions with a great deal of fat can appear bright.

Subcutaneous fat provides an example of this problem. It should have negative intensity in the opposed images but appears bright in the back in both Figures 4 and 5. As a consequence this tissue shows up in the water image rather than in the fat image where it belongs. The subcutaneous fat at the front does not show this problem. Breathing motions as large as the fat thickness probably average in enough water from deeper tissues to keep the intensity positive or near zero, avoiding this problem. The dark stains on the muscle surfaces in Figure 5, opposed image, are probably partial-volume effects also, the fat intensity being spread into muscle by slight subject motion.

An opposed image by itself may contain all the clinical information necessary without the need for comparison with an in-phase image. This image definitely contains spectroscopic information but calling it a spectroscopic image implies the existence of a one-point spectrum. This is certainly a new standard for economy of information.

The careful reader may notice that the water and fat images should not come out in perfect register. Both the excited fat and water have a proton Larmor frequency equal to that of the RF pulse. Because water and fat have different chemical shifts and the section selection gradient is on, the water plane and fat plane being imaged have slightly different positions along the gradient axis. This is no different in spectroscopy from ordinary imaging.

The warp gradient has no such effect but there is also misregistration in the direction of the read-out gradient. Since frequency is equated to position in image processing, spins with different frequencies appear to be in different places. This is true whether they have the same chemical shift and different positions, or the same position but different chemical shifts. In this work this offset is somewhat less than 1 pixel. Naturally this can be corrected easily if the offset is adjusted to a whole number of pixels. While that was not done here, in principle improved edge-definition is a free bonus of spectroscopy.

CONCLUSIONS

It is possible to do useful proton spectroscopy in an imaging mode on any commercial imager at fields at least as low as 0.35 Tesla. New images that result are water only, fat only, and water less fat. Sacrificing chemical shift resolution (spectra have only 2 or even 1 point) allows these images to be ob-

tained with little or no loss in spatial resolution, signal-to-noise ratio, or imaging speed.

These new images delineate most organs in the abdomen more clearly than conventional MR images.

Using spectroscopy, separate relaxation times can be obtained for tissue water and tissue fat, rather than just the weighted averages now obtained from images. Eliminating this weighted averaging eliminates a source of laboratory to laboratory variation in measurements as well as providing new parameters for tissue characterization.

Acknowledgments: The author thanks the MR groups at both the Mallinckrodt Institute and Siemens for technical help, W. A. Murphy, M.D., for suggestions on the manuscript, and M. Rowley for manuscript preparation. Before this work was undertaken, Drs. J. J. J. Ackerman, J. L. Evelhoch, and D. E. L. Jick kindly measured the homogeneous T2 of fat in a living mouse to determine whether fat imaging would be possible.

References

1. Lauterbur PC, Kramer DM, House WV, Chen C-N. Zeugmatographic high resolution nuclear magnetic resonance spectroscopy. Images of chemical inhomogeneity within macroscopic objects. J Amer Chem Soc 1975; 97:6866–6868.
2. Bendel P, Lai C-M, Lauterbur PC. ^{31}P spectroscopic zeugmatography of phosphorus metabolites. J Mag Res 1980; 38:343–356.
3. Cox SJ, Styles P. Towards biochemical imaging. J Mag Res 1980; 40:209–212.
4. Brown TR, Kincaid BM, Ugurbil K. NMR chemical shift imaging in three dimensions. Proc Natl Acad Sci USA 1982; 79:3523–3526.
5. Hall LD, Sukumar S. Chemical microscopy using a high-resolution nmr spectrometer. A combination of tomography/spectroscopy using either ^{1}H or ^{13}C. J Magn Reson 1982; 50:161–164.
6. Maudsley AA, Hilal SK. Perman WH, Simon HE. Spatially resolved high resolution spectroscopy by "four-dimensional" NMR. J Mag Res 1983; 51:147–152.
7. Pykett IL, Rosen BR. Nuclear magnetic resonance: *in vivo* proton chemical shift imaging. Radiology 1983; 149:197–201.
8. Hall LD, Sukumar S, Talagala SL. Chemical-shift-resolved tomography using frequency-selective excitation and suppression of specific resonances. J Magn Reson 1984; 56:275–278.
9. Hall LD, Sukumar S. A new image-processing method for chemical microscopy. J Magn Reson 1984; 56:326–333.
10. Edelstein WA, Bottomley PA, Hart HR, Smith LS. Signal, noise, and contrast in nuclear magnetic resonance (nmr) imaging. J Comput Assist Tomography 1983; 7:391–401.
11. Abragam A. Principles of nuclear magnetism. London: Oxford University Press, 1961: 33,34,58–63.
12. Droege RT, Wiener SN, Rzeszotarski MS, Holland GN, Young IR. Nuclear magnetic resonance: a gray scale model for head images. Radiology 1983; 148:763–771.
13. Edelstein WA, Hutchison JM, Johnson G, Redpath T. Spin warp NMR imaging and applications to human whole-body imaging. Phys Med Biol 1980; 25:751–756.
14. Hutchison JMS. NMR scanning: the spin warp method. In: Witcofski RL, Karstaedt N, Partain CL, eds. International symposium on nuclear magnetic resonance imaging. Bowman Gray School of Medicine, 1981: 77–80.
15. Allerhand A. Cochran DW. Carbon-13 Fourier-transform nuclear magnetic resonance. I. Comparison of a simple spin-echo procedure with other methods. J Amer Chem Soc 1970; 92:4482–4484.

Washington University School of Medicine
510 S. Kingshighway
St. Louis, MO 63110